

## **Suspension bridge response due to extreme vehicle loads**

Robert Westgate\*<sup>a</sup>, Ki-Young Koo<sup>b</sup>, James Brownjohn<sup>a</sup> & David List<sup>c</sup>

*<sup>a</sup>Department of Civil and Structural Engineering, University of Sheffield, Sheffield, United Kingdom; <sup>b</sup>Department of Civil Engineering, Kyungil University, Daegu, Republic of Korea; <sup>c</sup>Tamar Bridge and Torpoint Ferry, Plymouth, United Kingdom*

\*Corresponding author. Email: [r.westgate@sheffield.ac.uk](mailto:r.westgate@sheffield.ac.uk)

Correspondence details: 36/38 Victoria Street, Sheffield, South Yorkshire, S3 7QB, United Kingdom.

## **Suspension bridge response due to extreme vehicle loads**

A 269 tonne trailer travelled across the Tamar Suspension Bridge in October 2010, and the authors monitored the response of the structure to the load. The following investigation documents the deflection of towers and the deck during the vehicle's passage, as well as the change in cable tensions. This was achieved by studying monitored data from the bridge collected by accelerometers and strain gauges attached to the stay cables, as well as two Robotic Total Stations (RTS) that measured the deflection of the mid-span and the sway of the tower saddle. These results were subsequently compared to the response predicted by a Finite Element (FE) model of the bridge, indicating an accurate match. The FE model was also used to simulate the variation of the dynamic response of the structure, which suggests the natural frequencies vary depending on the vehicle's location to each mode shape's anti-nodes.

Keywords: bridges; bridges, cable-stayed; bridges, suspension; dynamics; site investigation; traffic engineering.

### **Introduction**

It is a rare opportunity to monitor the response of a bridge when it is loaded by a trailer that is significantly heavier than the standard design heavy vehicle. The passage of an extremely heavy vehicle provides an excellent chance to study the performance of a large civil structure with a known and controllable load and estimate its structural characteristics. While ambient vibration tests do not require large excitation devices like a heavy vehicle, conditions such as traffic are not controlled, and weather conditions such as temperature and wind may vary during the testing period so that system identification procedures have to be very sophisticated.

There are numerous papers that have described development of numerical models of a vehicle travelling across a bridge. The majority treat the vehicle as a series of spring-mass-dampers that are excited by the irregularities of the road (Green & Cebon, 1997; Guo & Xu, 2001; Haji-Hosseini & Bakhtiari-Nejad, 2010; Mulcahy,

1983; Xia, Xu & Chan, 2000). The resulting vehicle-structure interaction can lead to changes in the observed dynamic properties of the bridge (Kwon, Kim & Chang, 2005; Li, Su & Fan, 2003; Yang, 2004; Yang, Liao & Lin, 1995). There are also several documented site investigations monitoring the bridge deck vibration with excitation provided by a heavy vehicle (Calcada, Cunha & Delgado, 2005; J. Kim, Lynch, Lee & Lee, 2011; Lin & Yang, 2005; Mazurek & DeWolf, 1990; Paultre, Proulx & Talbot, 1995; Yin & Tang, 2011). A review by Paultre, Chaalal and Proulx (1992) showed that the mechanical properties of the vehicle affects the dynamic response of the bridge, when the two interact from the roughness of the bridge surface. However, these excitation frequencies lie between 2-5Hz for the bounce of the vehicle's body, and would have limited effect on bridge modes with lower frequencies.

The quasi-statically varying shape of cable supported bridges changes during the passage of a heavy vehicle, due to the flexible deck structure and redistribution of forces in the cables. During a controlled vehicle loading the deflections at certain points in the structure might be tracked via positioning systems, such as used on the Forth Suspension Bridge in the UK (Roberts, Meng, Brown & Andrew, 2006) and Batman cable-stayed bridge in New Zealand (Watson, Watson & Coleman, 2007).

It is suspected that the natural frequencies of the bridge structure change when the additional mass of the vehicle is large compared to the mass of the bridge deck. Kim, Jung, Kim and Yoon (2001) observed a change in the monitored natural frequencies of three bridges while under various traffic and heavy-vehicle loadings. However the variations experienced by the Namhae suspension bridge were very low, changing by only 0.01% at most. De Roeck, Maeck, Michielsen and Seynaev (2002) performed numerical simulations of a vehicle traversing a box girder bridge, and showed how the change in the natural frequency of the modelled structure depended on

the ratio of the vehicle's mass to the bridge. Law (2004) observed the first natural frequency of a simulated bridge decreasing as the vehicle moved towards its centre, the location of the vehicle affecting the dynamic characteristics of the structure, depending on the modal ordinate at the vehicle location.

The focus of this paper is a site investigation on the performance of Tamar Suspension Bridge during the passage of a heavily laden vehicle, which provided an opportunity to observe changes in response to a travelling concentrated mass, with an unusual ratio of vehicle and bridge weights. The objective of this investigation was to record the deflection of the bridge deck and towers, as well as to identify the dynamic behaviour of the additional stay cables.

A finite element (FE) model of the bridge is used to provide a prediction of these responses via a series of static and dynamic analyses for specific vehicle locations, which are compared with results obtained from the monitoring system. This investigation also uses the FE model to simulate the deviation of the suspension and stay cable tensions as the bridge reconfigured to adapt to the moving loads. Finally, the frequencies of the structure are simulated via the FE model, and compared with limited dynamic response data from the structure.

## **Site investigation on the Tamar Suspension Bridge**

### ***Bridge Details***

The Tamar Suspension Bridge has a 335m main span and two 114m side spans, with a road structure that consists of a 4.9m deep steel truss and a steel orthotropic deck. In addition to the 38cm diameter suspension cables, there are also eight pairs of stay cables (P3, P1, ... , S3) that contribute to the vertical support of the truss. The concrete towers are 73.2m tall with the bridge deck supported halfway, and are seated on caisson

foundations. The width of the bridge, including the two 6.0m wide cantilevered lanes, is 27.2m.

### ***Test details***

Full Scale Dynamics Ltd (FSDL), a University of Sheffield spin-off company founded by Vibration Engineering Section (VES) researchers was contracted by the Tamar Bridge and Torpoint Ferry Joint Committee operators to record the deformation of the bridge while a 151 tonne electrical transformer for a power station was transferred from Plymouth to Saltash.

The trailer carrying the transformer crossed the bridge during the early hours of October the 31<sup>st</sup> 2010, and FSDL were on site to monitor and study bridge behaviour. Due to the abnormal bulk of the trailer, almost the same weight as a traffic jam across the main span, the bridge was closed to normal traffic.

The performance of the bridge is currently being recorded as part of an ongoing long-term monitoring project, and has been instrumented with a variety of sensors to determine variations in quasi-static and dynamic responses (Koo, Brownjohn, List & Cole, 2012). The general arrangement of the sensors used for the site investigation is shown in Figure 1.

Two robotic total stations (RTS) located at the Tamar Suspension Bridge office on the Plymouth side of the bridge traced the position of two reflectors: one monitored the reflector at the top of the northern Saltash tower; the other tracked the reflector at the centre of the main span. The RTS unit is a Leica TCA1201, and has an accuracy of 2mm + 2 ppm when measuring distance. The reflector on the Saltash tower reflector is 650m from the RTS, which may have up to 3.3mm error when measuring the distance, and 3.2mm error in the vertical and lateral directions.

Accelerations were collected from a set of uni-axial QA700 and QA750 force-balance type accelerometers. These are attached to two of the stay cables, the northern and southern cable at location P4, aligned perpendicularly to capture its transverse and vertical movements. Signals from the deck accelerations at mid-span were available, but were unusable due to signal spikes and very poor signal to noise ratio.

A long-term monitoring system installed on the bridge by Fugro Structural Monitoring is used to determine the tensions in the stay cables, as well as ambient weather conditions (wind speed, bridge and air temperature, humidity), which were constant and benign for the short duration of the vehicle transit. The load in the stay cables are measured by a pair of resistive strain gauges attached to the main tensioning bolts at the deck anchor points; one gauge is aligned axially to the cable, while the other measures hoop strain and compensates for temperature change.

Since there was an interest in capturing as much of the bridge's behaviour as possible, the sampling rates were increased for the sensors on the VES system: the accelerometers data were sampled at 32Hz, and the RTS measurements at 3Hz. Sensors on the Fugro monitoring system remained at their programmed sampling rate of once every 10 seconds since such responses are not expected to change significantly over that period.

Figure 2 shows the longitudinal dimensions for the transport arrangement of the trailer, which was pulled by two FAUN tractors with an 8x8 wheelbase, one at either end. Wheelbase and axle weights were approximated from provided technical drawings and datasheets from similar tractor models (Inter-Commerz, 2008). It is assumed the trailer supported 16.9 tonnes per axle with a 1.5m wheelbase along the length of the trailer, and 2.5m axle track. The container for the transformer was elevated clear from

the road, providing a 15.2m unloaded gap along the deck. The total mass, trailer and tractors, was approximately 269 tonnes.

The designed loading capacity of the Tamar Suspension Bridge is 1865 tonnes distributed along the whole span of the bridge, or a single 180 tonne vehicle if two of the lanes are closed off to other traffic. Prior to the site investigation AECOM, the consultant engineers, checked if the bridge could support a 295 tonne trailer with two 46 tonne trucks, and concluded the test could be run safely.

### ***Finite element model***

Prior to the measurements, an FE model of the bridge was used to determine which of the reflectors on the bridge best demonstrated the response of the bridge (Westgate & Brownjohn, 2010), as well as to establish an approximation for the expected magnitude of the deflections. Following the site investigation the FE model was later used as a comparison to the monitored results, as well as predicting related responses that were unrecorded.

The FE model was created in ANSYS 12.1 and consists of 16000 nodes and 40000 elements. The truss members were modelled as either BEAM4 or BEAM44, while plate elements found in the deck and the towers were modelled as SHELL63, all of which provide six degrees of freedom at each node. The cables and hangers were modelled as LINK10 with the “tension only” option activated, so that the elements provided zero stiffness under compressive loads.

The main span and Plymouth side span are connected via the deck and cantilevers, while there is an expansion gap near the Saltash tower to allow longitudinal movement. Some longitudinal stiffness has been provided at the expansion gap by a linear spring element (COMBIN14) to represent some rigidity caused by friction at the bearings. Long-term monitoring of the bridge has shown that the bridge span moves

towards the expansion gap, rather than out towards the side towers. As a result, the longitudinal and rotational spring elements at the side towers are much stiffer than at the expansion gap. The foundations are highly stiff; their caissons are 10.2m below the ground and positioned on solid rock, so it was reasonable to model the towers as fully-fixed at their bases.

Due to the slow speed of the trailer the study was performed as a series of static analyses for each location of the vehicle. Each static analysis identified the changes in the bridge's configuration, such as its deformed shape and variations in the tensions of the hangers, suspension and stay cables. These effects were accounted for in the subsequent modal analysis, in order to determine variations in the bridge's dynamic properties. To illustrate the passage of the vehicle as smoothly as possible, the deck was meshed with span-wise divisions every 0.5m. The dimensions of the vehicle model were rounded to comply with this mesh length. The vehicle model was treated as a series of 22 travelling masses acting on each axle: 4 for each tractor and 7 for each trailer. The parameters used in the model are listed in Table 1. Since the trailer travelled along the central lane of the bridge, these masses were applied to the nodes along the middle of the deck elements.

The timescale in the FE model simulation was calibrated with the site investigation via the peak deflections observed in the monitored data, the Saltash tower's deflections in particular provided a suitable match. These recorded times were also used to approximate the speed of the vehicle, assumed to be constant, which was 5 miles per hour ( $\sim 2.24\text{m/s}$ ), giving a time between mesh nodes of 0.22 seconds. The approximate times when the centroid of the trailer passed particular locations was determined by the calibrated FE model results, and are presented in Figure 3.



## **Quasi-static response of the bridge to the trailer**

### ***Monitored and predicted deflection of the mid-span***

Once the data for the site investigation and quasi-static analyses on the FE model were collected, the two were compared to validate the response of the modelled structure.

Figure 4 shows the vertical deflection of the mid-span over the period of the site investigation, for both responses monitored from the structure and simulated in the FE model. The ticks on the horizontal axis are the time when the centre of the trailer is near to the location of the main and side towers, shown previously in Figure 3. The shape of the lines demonstrates the significant negative vertical deflection when the trailer is on the main span, reaching its peak at mid-span before returning to its previous state. The mid-span deflects vertically upwards when the trailer is on the side spans. Since the Saltash side span is not connected to the main span, yet the response is similar for both sides of the bridge, the continuity has to be provided via the deflection of the towers and the suspension cables, which pull the spans upwards when the neighbouring spans deflect downwards. As the trailer approaches the towers the vertical deflection returns to 0. An interesting feature is the pair of acute troughs in the FE model time series results; the gap created when the 15.2m of unsupported space between the trailers passes across the mid-span of the bridge. The slight spike in the monitored results might suggest this response was also observed on the actual structure.

The longitudinal response of the mid-span in Figure 5 shows that as the trailer enters the bridge, the mid-span moves east towards Plymouth. This reaches a peak at approximately 06:29.45, when the trailer is close to a quarter length of the main span. This mid-span moves back west and passes back through its original displacement when the trailer arrives at mid-span, then continues in the westerly direction as the vehicle travels on the Saltash side of the bridge. This 'S' shaped response is a result of the

changing curvature of the bridge: when the trailer is at quarter span the bridge deck sags asymmetrically, and as a consequence the mid-span moves towards the depression created by the trailer.

The mid-span also moves a little when the vehicle is on a side-span, as shown by a minor peak in the monitored results at 06:29. This appears to be due to the longitudinal continuity of the bridge deck at the Plymouth tower, since this response effects appears only very weakly when the vehicle is on the Saltash side span, beyond the expansion gap.

### ***Quasi-static tower response to the trailer load***

The easterly deflection of the Saltash towers shown in Figure 6 resembles the longitudinal displacements at mid-span. Once the trailer moves onto the main span, the deflection of the deck causes both tower tops to move inwards. The towers revert to their original state once the trailer moves beyond the main span. The towers also deflect in the opposite direction once the trailers moves onto the Saltash side span, for the same reason. A similar but reversed response is exhibited on the Plymouth towers, which were not monitored.

### ***Changing cable tensions***

Since the deck deflects vertically and the towers sway as the trailer crosses the bridge, changes in the suspension and stay cables tensions, which link the tower and the deck, were expected. Figure 7 shows that the tensions of the stay cables connected to the main span also peak when the trailer is near the mid-span. The initial tensions differ slightly between the two since the FE model is calibrated to long-term monitoring data, and the tensions in the stay cables vary depending on their temperature. The peaks in the stay cable tensions occur at the same time as the trailer passes their connection to the deck,

indicating a direct relationship to the location of the trailer on the bridge. The largest changes in stay cable tension are for the cable closest to the towers, i.e. S2 and P2, although the change in tension for S2 is half the size in the monitored results than the simulated results. The tensions in the cables also relax when the trailer is at the opposite main span location, due to upwards deck curvature.

For tensions of the stay cables connected to the side spans, shown in Figure 8, the P1 and S1 stay cable tensions also peak when the trailer is situated at their deck connection. In addition, a smaller peak forms when the trailer is on the main span, which may be attributed to the main towers being pulled towards the main span. Stay cables S3 and P3 slacken when the trailer is on their connecting side span since, unlike the other six pairs of stay cables, they anchor their connected tower saddle directly to the base of a side tower and are only affected by tower deflection. Similarly their tensions increases when the trailer is loading the main span since the towers are deflected towards the main span. There is also a slight crest in the tensions of stay cable P1 in the simulated data when the trailer is on the main span, which does not have an analogue for S1. The lack of crest in the Saltash tensions is due to the expansion gap at the Saltash tower, which gives the side span more freedom to expand longitudinally and accommodate the sway of the tower. The crest in the S1 tensions appears in the monitored data, however, since the additional cable tensions are transferred from S2. This accounts for the differing response of stay cables S1 and S2 to the simulated data.

It was assumed that the stay cable tensions may affect the suspension cable tensions, since the two are related by the horizontal force equilibrium at the saddles. Figure 9 indicates that when the side spans are loaded, the predicted tensions in the loaded side-span's suspension cables reduce, as a result of the tower deflection caused by the stay cables. This differs from the response predicted by FE model of the bridge

without the stay cables in Figure 10, where the side-span suspension cable tensions tauten when the same side-span is loaded.

Similarly the presence of stay cables in the structure causes the side-span suspension cables tensions to peak when the vehicle is at the quarter points of the main span, rather than halfway. This is produced by the suspension cables responding to the increasing main span stay cable tensions. The difference in magnitude of the tensions on Plymouth side span compared to Saltash side span is due to the different stay cable tensions on either tower, which were present in the unloaded structure.

The tension variations for the suspension cable at the two main span quarter-points are identical, despite the longitudinal asymmetry provided by the expansion gap. Thus the change in suspension cable tension is only dependent on the distance of the vehicle from the mid-span. Similarly the quarter span tensions are the same shape as the tensions at mid-span, since the majority of the total vertical load on the suspension cables is supported by the horizontal component of tension; the quarter span tensions being larger due to inclination to the horizontal.

### **Variation in dynamic properties of the bridge**

So far the static deflections of the structure have been observed, along with variations in cable tensions depending on the location of the vehicle. The trailer mass itself is large compared to the bridge: the 335m main span of the structure weighs approximately 3190 tonnes, making the vehicle/bridge mass ratio greater than 8%. It seems credible that both the changing tension stiffness and the immense travelling mass would have a significant effect on the dynamic properties of the bridge. The study is limited to effects of the additional mass along with changes in the bridge configuration and tensions of main cables and additional stays. The effect of vehicle-structure interaction was considered, but the additional response was negligible due to the relatively low

frequencies of the global vibration modes studied.

Since the signals from the deck accelerometers were too corrupted, the experimental dynamic properties of the bridge during the investigation are not acceptable for publication, unfortunately. For the simulated properties determined from the FE model, Table 2 show that the changes of the natural frequency for the first six modes may be substantial. Predicted changes in the natural frequencies are 50 times larger than those documented on the Namhae Suspension Bridge (Kim et al., 2001), despite having similar span lengths, suggesting that the large mass of the trailer has a considerable effect on the dynamic response. The natural frequencies may rise as well as fall, depending on the relative effects of the extra mass and the extra tension. For most the observed modes, the largest variation tends to take place towards the centre of the main span, however on modes VA1 and VS2, where the mode shape consists of two or more curves on the main span, the highest variation is when the trailer is off-centre; for VA1 this is at quarter span on the Plymouth side, while on VS2 it is on the Plymouth side span.

### ***Changes in the natural frequencies***

The variation in the natural frequencies is dependent on the location of the trailer along the length of the span, as shown by Figure 11, the origin for the ordinate system lies at the Plymouth side tower. The troughs and peaks in the frequencies of the first three modes occur when the trailer is over the anti-node of the mode shape. For example, since the first two global mode shapes, VS1 and LS1a, are symmetric and resemble a half-sine wave, their frequencies peak when the trailer is at mid-span. Likewise the third mode, VA1, is the first vertical anti-symmetric mode and resembles a full sine wave, and the greatest effect is when the trailer is near the quarter span of the bridge. The larger drop in the frequency of VA1 is on the Plymouth side of the bridge, which is due

to the continuity of the main span to the side span. It is observed that the frequency of vertical mode shapes falls as the additional mass of the trailer moves towards the part of the structure with the largest modal ordinate. The frequencies of lateral modes relate more to the changes in cable tensions, and will increase as a result of tension stiffening more than they decrease due to the added mass.

The behaviour for the next three modes in Figure 12 shows that the first torsional mode, TS1, has a similar response to the second lateral mode, LS1b, which also has a slight axial rotation. The curve of the lines for these two modes is shallower, suggesting little reaction to the location of the vehicle. This response seems credible, since the trailer model is positioned along the centre lane of the bridge, and is not likely to cause axial rotations.

The most striking effect is the frequency variation for the second vertical symmetric mode, VS2. The three central troughs are formed when the tractor is at quarter spans or the mid-span, much like the mode shape. Frequency changes when the vehicle is on the side span seem disproportionately large compared to the mode shapes, although mode shape ordinates on the Plymouth side span are larger than those on the Saltash side span, as are the frequency changes. The differing response when the trailer is on the Plymouth side span compared to the Saltash side is due to the discontinuity of the deck structure at the Saltash expansion gap, and the participation of the side spans in the VS2 mode shape. When the vehicle is on the Plymouth side span, changes to the modal displacements, the rotations at the Plymouth tower in particular, are transferred to the main span. When the vehicle is on Saltash side span, however, the connectivity to the main span is only provided by the suspension and stay cable tensions.

### ***Changes in the modal displacements of modes VS1 and VS2***

Figure 13 shows the change of the absolute modal displacements for the first vertical

symmetric mode of the bridge, as the vehicle travels from one longitudinal location to another. The results show that the mode shape barely changes until the trailer is on the main span, between the 113m and 448m longitudinal coordinate. On the main span from Plymouth the modal displacement decreases until the trailer reaches the mid-span, the anti-node of the mode shape, before rising again as it travels to Saltash. The 'S' shaped curve that is appearing on the main span in the plan view suggests that the mode shape is asymmetrically curving towards the half of the main span supporting the vehicle. This response shares some similarities to the static deformations, where the mid-span moves longitudinally in the direction of the trailer.

Figure 14 also shows the change in absolute modal displacements, but for the second vertical symmetric mode. This mode was selected due to the high variation in frequency and modal mass when the Plymouth side span was loaded by the trailer, which may also relate to changes in the mode shapes. When the trailer is travelling across the mid-span the isometric plot indicates the modal displacements are fluctuating with crests forming at the anti-nodes, much like the results seen previously for the first vertical mode.

While the trailer is on the main span, the mode shape is mostly similar to its shape when the bridge is unloaded, the only variation is a reduced modal deflection at mid-span when the trailer is at the centre of the bridge. However, an interesting change to the mode shapes occurs when the trailer is located at the centre of a side span, which is visible in the plan view of the plot. Two vertical bands form when the trailer is located near the 56 and 501m longitudinal coordinates of the bridge, the modal displacements differing significantly compared to other locations of the structure. This indicates that the mode shape of the bridge is altered, with the largest modal deflections occurring on the side-spans instead of the main span. The largest displacement on the

Plymouth side span also corresponds to the large change in natural frequency for this mode while the vehicle mass is located upon it.

### ***Relating the frequency changes to the modal displacements***

The following pairs of figures showing two views of a three-dimensional plot aim to link the change in frequency  $\Delta f$  to the vehicle location  $x$  and mode shape ordinate  $\phi$ , for modes VS1 and VS2. The left-hand plots, Figure 15 and Figure 17, show the absolute value of the mass-normalised vertical mode shape ordinate  $\phi$  for the mode versus span-wise location  $x$ . In Figure 16 and Figure 18 for each vehicle location  $x$  the change in natural frequency  $\Delta f$  previously calculated is plotted against the modal ordinate for location  $x$ . A colour bar indicating the location  $x$  for the trailer load is also provided to help understand the changes as the vehicle moves from one half span to the other.

A linear relationship between frequency change and absolute modal displacement might be expected, for VS1 it comes close to that. While the short lines in Figure 16 the side spans show a linear relationship, they also have steeper slopes i.e. the first natural frequency barely changes when the trailer is on the side span.

The results for the second vertical symmetric mode are also presented here to test whether similar linear relationships occur when the mode shape for the main span consist of more than one sinusoid. Figure 18 shows that the relationships when the vehicle is at the quarter span of the main span follow similar gradients, although the open loops indicate the relationships are not as tight as the previous VS1 results. Likewise the change in frequency when the side-spans are loaded does not follow the same relationship to the mode shape like the main spans. In particular when the Plymouth side span is loaded the natural frequency change for this mode is large,



despite the modal displacements on the Plymouth side-span being slightly smaller than those on the main span. This effect is due to the Plymouth side span's continuity with the main span, which links their modal responses.

### **Stay cable accelerations**

As well as quasi-static effect described in previous sections, the time series for the vertical and transverse accelerations of the North and South P4 stay cables were also available, as shown in Figure 19. The cable accelerations begin to grow once the trailer moves onto the main span, at 06:29.10, and reach maximum amplitude of  $0.4\text{m/s}^2$  with the vehicle at mid-span. Beyond that point the accelerations decrease, although the cable accelerations are larger when the vehicle is on the Saltash side span compared to when it is on the Plymouth side span.

The stay cable accelerations were further processed to see how the cables natural frequencies changed as the vehicle travelled across the bridge, as presented in the spectrogram of Figure 20. The average tension in the two stays cable before the bridge was loaded was  $2269\text{kN}$ , and according to the long-term monitoring data would have a natural frequency of approximately  $0.98\text{Hz}$ . Consequently the strong bands at  $1\text{Hz}$  intervals in the spectrogram correspond to the second to sixth harmonics of the cable.

The frequency of the cable increases at 28 minutes, which corresponds to the time when the P4 tensions increase, and the vehicle is near its deck connection.

Assuming that the change in frequency is a result of the  $402\text{kN}$  tension rise of the P4 stay cable, and taking the cable length as  $110\text{m}$  and its mass as  $58.4\text{kg}$  per metre,

Humar's equation for the natural frequencies of a cable can be used to determine the theoretical rise for the  $n$ th frequency,  $f_n$  (Humar, 1990):

$$\left(\frac{f_n}{n}\right)^2 = \frac{T}{4mL^2} + \frac{n^2\pi^2 EI}{4mL^4} \quad (1)$$

where  $T$  is the tension in the cable,  $m$  is cable mass per unit length,  $L$  the effective length of the cable, and  $E$  and  $I$  the Young's modulus and second moment of area for the cable, respectively.

For the first mode, the rise in frequency is approximately 0.144Hz, assuming the elastic stretch of the cable is negligible. Since the frequencies for higher order harmonic are almost multiples of the first mode's frequency, doubling this result appears to correspond with the rise near 2Hz for the second harmonic. The changes in the fifth and sixth harmonics are the most visible in the P4SV spectrogram, demonstrating that the increase in frequency also multiplies for the higher order harmonics.

## **Conclusions**

In this investigation, variations were observed in the static deflections and dynamic response of the Tamar Suspension Bridge during crossing of a 269 tonne vehicle. The study uses data collected from the site investigation, as well as the simulations using an FE model of the bridge. The static analyses using the FE model have provided a satisfactory mirror of the observed behaviour, with an acceptable match to displacements recorded by the two total stations.

The deck vertical displacements and movement of the tower observed corresponded well with the finite element model predictions. The stay cable tensions peaked when the trailer was near their connection to the deck, the largest response being observed in the stay cables with the steepest inclination. Variations in the suspension cable tension are observed as the vehicle travels across the entire span of the bridge.

The frequencies simulated in the FE model varied according to trailer locations, with the largest variations appearing on the first two vertical symmetric modes. Similar changes were also exhibited in the mode shapes of the structure. In particular the dynamic properties of the second vertical symmetric mode change considerably when the trailer is on the Plymouth side span. The largest changes to a mode natural frequency correspond to the vehicle being located on the anti-nodes of its mode shape.

The accelerations from a pair of stay cables were also observed during the monitoring, and demonstrated an increase in natural frequency for several harmonics when the trailer travelled close to its deck connection. This variation was attributed to the increase in stay cable tension recorded for the structure.

## References

- Calcada, R., Cunha, A. & Delgado, R. (2005). Analysis of Traffic-Induced Vibrations in a Cable-Stayed Bridge. Part I: Experimental Assessment. *Journal of Bridge Engineering*, 10(4), 370–385.
- De Roeck, G., Maeck, J., Michielsen, T. & Seynaeve, E. (2002). Traffic-induced shifts in modal properties of bridges. *IMAC-XX: Conference & Exposition on Structural Dynamics* (pp. 630–636).
- Green, M. F. & Cebon, D. (1997). Dynamic interaction between heavy vehicles and highway bridges. *Computers & Structures*, 62(2), 253–264.
- Guo, W. H. & Xu, Y. L. (2001). Fully computerized approach to study cable-stayed bridge-vehicle interaction. *Journal of Sound and Vibration*, 248(4), 745–761.
- Haji-Hosseini, A. & Bakhtiari-Nejad, F. (2010). Vibration analysis and control of a bridge under a heavy truck load. *2010 International Conference on Mechanical and Electrical Technology* (pp. 195–200). IEEE.
- Humar, J. L. (1990). *Dynamics of structures* (1st ed.). Prentice-Hall, Inc.
- Inter-Commerz. (2008). Faun “Elephant SLT 50 8x8 + 8x0 datasheet. Retrieved September 15, 2011, from [http://www.inter-commerz.com/uploads/tx\\_ttproducts/datasheet/Faun\\_Elephant\\_SLT\\_50\\_8x8\\_8x0\\_ENG.pdf](http://www.inter-commerz.com/uploads/tx_ttproducts/datasheet/Faun_Elephant_SLT_50_8x8_8x0_ENG.pdf)







- Kim, C.-Y., Jung, D.-S., Kim, N.-S. & Yoon, J.-G. (2001). Effect of vehicle mass on the measured dynamic characteristics of bridges from traffic-induced vibration test. *Proceedings of SPIE, the International Society for Optical Engineering* (Vol. 4359, pp. 1106–1111). Society of Photo-Optical Instrumentation Engineers.
- Kim, J., Lynch, J. P., Lee, J.-J. & Lee, C.-G. (2011). Truck-based mobile wireless sensor networks for the experimental observation of vehicle–bridge interaction. *Smart Materials and Structures*, 20(065009).
- Koo, K., Brownjohn, J. M. W., List, D. I. & Cole, R. (2012). Structural health monitoring of the Tamar suspension bridge. *Structural Control and Health Monitoring*, 1–17.
- Kwon, S.-D., Kim, C.-Y. & Chang, S.-P. (2005). Change of Modal Parameters of Bridge Due to Vehicle Pass. *IMAC-XXIII: Conference & Exposition on Structural Dynamics - Structural Health Monitoring* (pp. 283–290).
- Law, S. S. (2004). Dynamic behavior of damaged concrete bridge structures under moving vehicular loads. *Engineering Structures*, 26(9), 1279–1293.
- Li, J., Su, M. & Fan, L. C. (2003). Natural Frequency of Railway Girder Bridges under Vehicle Loads. *Journal of Bridge Engineering*, 8(4), 199–203.
- Lin, C. & Yang, Y.-B. (2005). Use of a passing vehicle to scan the fundamental bridge frequencies: An experimental verification. *Engineering Structures*, 27(13), 1865–1878.
- Mazurek, D. F. & DeWolf, J. T. (1990). Experimental Study of Bridge Monitoring Technique. *Journal of Structural Engineering*, 116(9), 2532–2549.
- Mulcahy, N. L. (1983). Bridge response with tractor-trailer vehicle loading. *Earthquake Engineering & Structural Dynamics*, 11(5), 649–665.
- Paultre, P., Chaalal, O. & Proulx, J. (1992). Bridge dynamics and dynamic amplification factors - a review of analytical and experimental findings. *Canadian Journal of Civil Engineering*, 19(2), 260–278.
- Paultre, P., Proulx, J. & Talbot, M. (1995). Dynamic Testing Procedures for Highway Bridges Using Traffic Loads. *Journal of Structural Engineering*, 121(2), 362–376.
- Roberts, G. W., Meng, X., Brown, C. J. & Andrew, A. (2006). Measuring the movements of the Forth Road Bridge by GPS; lorry trials. In A. Kumar, C. J. Brown & L. C. Wrobel (Eds.), *The First International Conference on Advances in Bridge Engineering. Bridges - Past, Present and Future* (UK, Uxbrid., Vol. 2, pp. 28–36).
- Watson, C., Watson, T. & Coleman, R. (2007). Structural Monitoring of Cable-Stayed Bridge: Analysis of GPS versus Modeled Deflections. *Journal of Surveying Engineering*, 133(1), 23–28.

- Westgate, R. J. & Brownjohn, J. M. W. (2010). Development of a Tamar Bridge Finite Element Model. *Proceedings of IMAC XXVIII*. Jacksonville, FL, USA: Springer New York.
- Xia, H., Xu, Y. L. & Chan, T. H. T. (2000). Dynamic interaction of long suspension bridges with running trains. *Journal of Sound and Vibration*, 237(2), 263–280.
- Yang, Y.-B. (2004). Extracting bridge frequencies from the dynamic response of a passing vehicle. *Journal of Sound and Vibration*, 272(3-5), 471–493.
- Yang, Y.-B., Liao, S.-S. & Lin, B.-H. (1995). Impact Formulas for Vehicles Moving over Simple and Continuous Beams. *Journal of Structural Engineering*, 121(11), 1644–1650.
- Yin, S.-H. & Tang, C.-Y. (2011). Identifying Cable Tension Loss and Deck Damage in a Cable-Stayed Bridge Using a Moving Vehicle. *Journal of Vibration and Acoustics*, 133(021007).

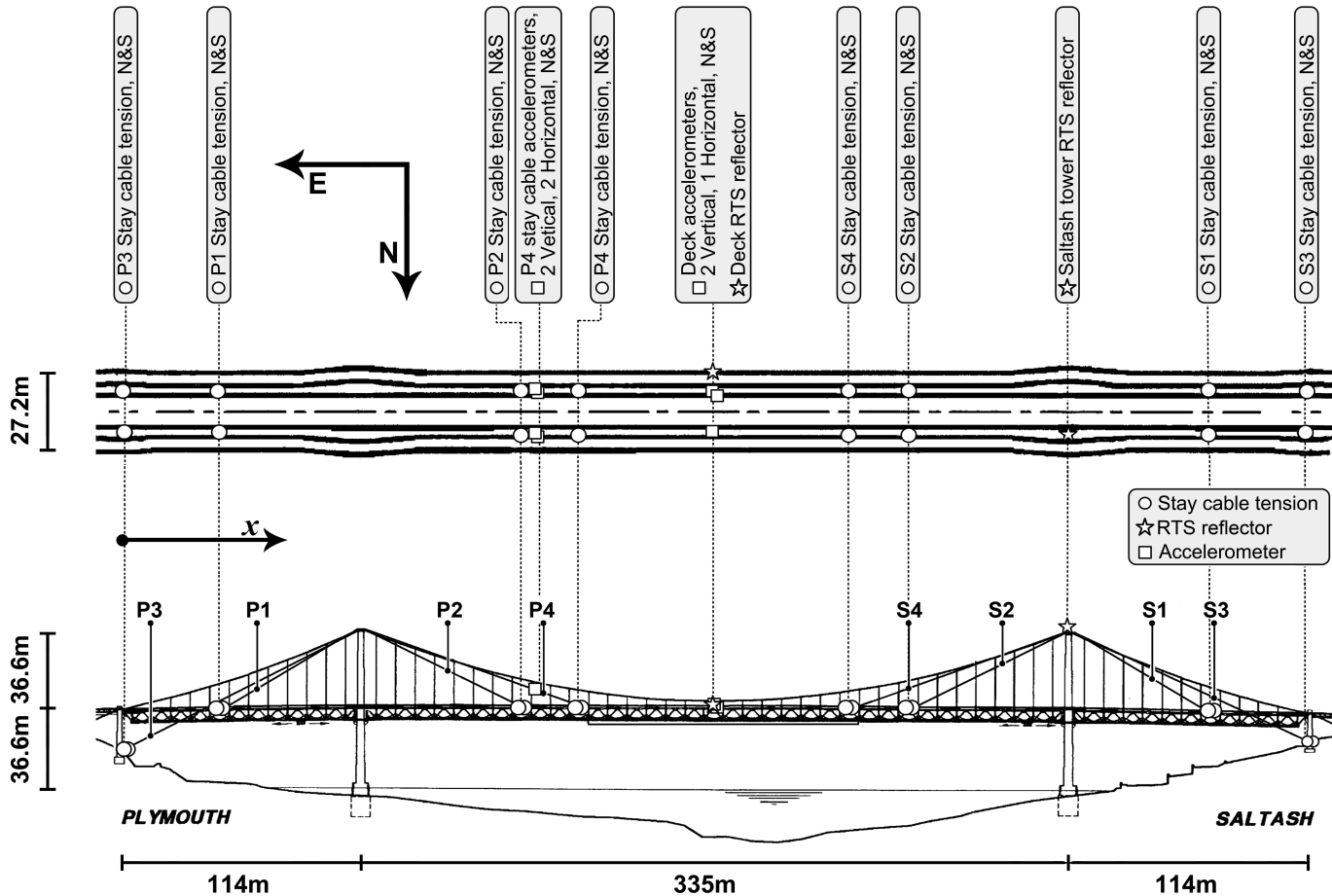
Table 1: Parameters for modelling the tractor-trailer model.

<b>Vehicle body</b>	<b>Symbol used in Figure 2</b>	<b>Mass of body</b>
Tractor on front axles	A	3232.5kg
Tractor on rear axles	B	1667.5kg
Trailer upon each axle	C	16860.0kg

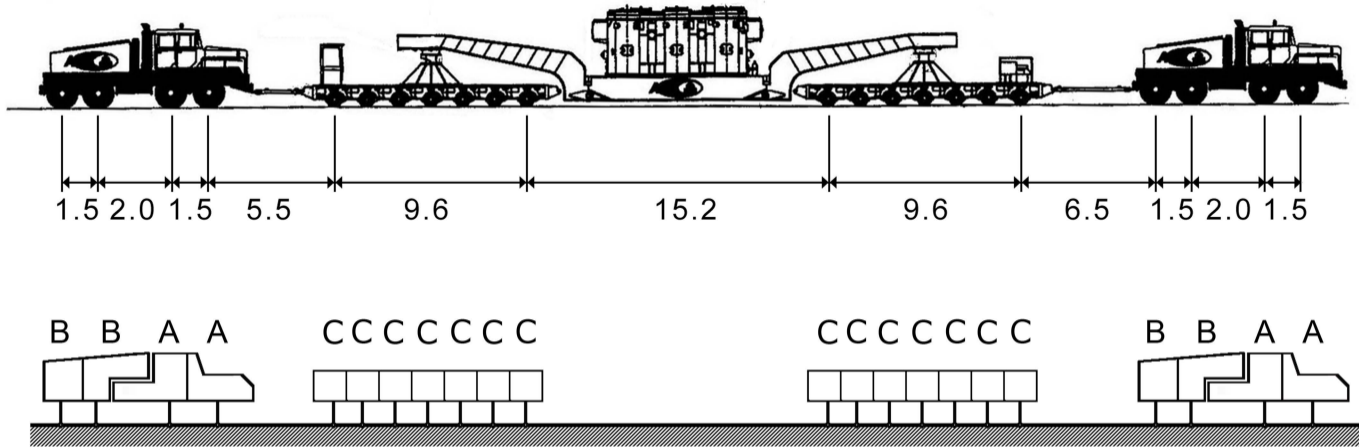
Table 2: Change in FE simulated frequency.

Mode	Shape	Original Frequency, Hz	Change to Frequency, Hz	Variation, %	Ordinate of trailer load, m
1	 VS1	0.389	-0.0282	-7.2	280 (Mid-span)
2	 LS1a	0.480	+0.0230	+4.8	281 (Mid-span)
3	 VA1	0.533	-0.0273	-5.1	190 (Plymouth quarter-span)
4	 LS1b	0.751	+0.0095	+1.3	286 (Mid-span)
5	 TS1	0.772	+0.0075	+1.0	284 (Mid-span)
6	 VS2	0.841	-0.0576	-6.9	56 (Centre of Plymouth side-span)

Note: where VS1 is the first symmetric vertical mode, LS1a the first symmetric sway mode (with more cable activity than deck), VA1 the first anti-symmetric vertical mode, LS1b another first-order symmetric sway mode (with more deck activity than LS1a), TS1 the first symmetric torsional mode, and VS2 the second symmetric vertical mode.







1.5 2.0 1.5 5.5 9.6 15.2 9.6 6.5 1.5 2.0 1.5

B B A A C C C C C C C C C C C C C C C C B B A A

